P. Li

X-ray Microtomographic Characterization and Quantification of the Strain Rate Dependent Failure Mechanism in Cenosphere Epoxy Syntactic Foams**

By *Ruoxuan Huang*, *Peifeng Li*,* *Zhiyong Wang* and *Tong Liu*

[*]   *Dr. R. Huang, Prof. P. Li, Dr. Z. Wang*

School of Mechanical and Aerospace Engineering, Nanyang Technological University,

50 Nanyang Avenue, Singapore, 639798

Email: peifeng.li@ntu.edu.sg

Dr. T. Liu

Singapore Institute of Manufacturing Technology, Singapore, 638075

P. Li

Abstract

This work investigates the failure mechanism in cenosphere epoxy syntactic foams at the quasi-static and dynamic strain rates. Split-Hopkinson pressure bar experiments are controlled to stop dynamic deformation of the foams at various strain stages. The internal microstructure at each strain is characterized in the x-ray microtomography and compared to the microstructure in the foams deformed quasi-statically. The microscopic observations reveal that the failure process in syntactic foams at the low and high rates is dominated by the crushing of cenospheres and the cracking of the epoxy matrix. However, the mechanism of failure in the foam is significantly affected by the strain rate. Compared to quasi-static compression, macro-cracks form earlier in the matrix at dynamic rates and can propagate to split cenospheres. The volume of the damage as defined by the failure of both cenospheres and the matrix is calculated from the x-ray microtomographic images. It is found that the damage can be quantitatively related to the strain and the strain rate using an empirical equation.

Keywords: Syntactic foams; Dynamic behavior; Strain rate; Failure; X-ray tomography.

Syntactic foams are the composite material made of hollow microspheres dispersed in the polymer matrix.[1] The foam becomes increasingly used in automotive components due to the advantages such as lightweight, high specific stiffness/strength and excellent energy dissipation capacity. In particular, cenosphere fillers produced as the by-product of coal combustion have been used to develop the low cost syntactic foam. The application in the components motivates the research on evaluating the mechanical behavior of the foam at various loading rates.

A large number of investigations focused on bulk mechanical properties and the associated failure mechanism in syntactic foams subjected to various loads at quasi-static strain rates.[2-9] The characteristics of cenosphere fillers such as the volume fraction and the size have the impact on the low rate behavior of the foam.[4,8-11] The mechanical behavior is also significantly affected by the applied strain rate. Recently, more research efforts have been made to explore the high strain rate response of the foam.[10,12-20] Dynamic properties of syntactic foams are affected by the geometry and volume fraction of hollow microspheres.[13-16] The treatment of hollow microspheres can improve their interfacial adhesion to the epoxy matrix and thus the impact properties of the bulk foam, especially the strength.[10] Pellegrino et al. reported the glass microballoon polyurethane syntactic foam possesses higher strain rate sensitivity in tension compared to compression.[17] However, very little research has focused on the microscopic failure mechanism of syntactic foams subjected to dynamic loads.

The post-test scanning electron microscopic (SEM) [12,21,22] and x-ray microtomography (μXT) [18] examination on deformed specimens was commonly used to characterize dynamic failure features in syntactic foams. Li et al. inspected the fracture surfaces of glass microballoon syntactic foams subjected to the low and high

rate compression and elucidated the effect of the failure on the bulk strain rate dependency of the foam.[12] Nevertheless, the mechanism of high rate failure process in the foam was rarely studied in terms of the loading history. Moreover, there is a lack in the quantitative analysis of the damage evolution in syntactic foams as a function of strain rates.

The aim of this work is to investigate the failure mechanism in cenosphere epoxy syntactic foams at different strain rates and to quantify the evolution of damage (failure in the foam). The syntactic foam specimens were deformed to various strain stages in the quasi-static (0.003 s^{-1}) and dynamic (3000 s^{-1}) compression experiments. The μXT was then performed to characterize the internal microstructural change of the foams at each strain. An empirical constitutive equation was developed to quantitatively relate the damage to the strain and the strain rate.

Bulk Compressive Behavior at Different Strain Rates: In the SHPB compression of cenosphere epoxy syntactic foams, the incident, reflected and transmitted strain waves as measured in the bars (Figure 1(a)) were used to calculate the stress and strain rate histories in the specimen (Figure 1(b)). The strain rate was approximately constant (3000 s^{-1}) during the dynamic compression. It should be noted that the force equilibrium at the two ends of the specimen was established in the early stage of deformation (i.e., after ~30 μs).[23] Figure 2 shows the typical compressive stress–strain curves of cenosphere epoxy syntactic foams at the quasi-static and dynamic strain rates. A good repeatability in stress was achieved in the tests at each rate. The bulk stress–strain curves are similar in shape at both the low and high rates, and can be categorized into three regions (Figure 2). The initial, approximately linear region corresponds to the elastic deformation. The peak stress (σ_{pk}) then occurs and is followed by a drop in the stress. The subsequent plateau region is characterized by the

nearly constant stress (i.e., plateau stress σ_{pl}). Both the peak and plateau stresses are the main characteristics of the foam.[2,12] In the densification region, the foam is compressed into the bulk material and thus the stress increases rapidly.

The bulk stress of the syntactic foam is affected by the strain rate despite the similarity in the shape of the low and high rate stress–strain curves (Figure 2). For instance, the peak and plateau stresses at dynamic rates are 2–3 times higher than those at the quasi-static rates. As summarized by Li et al., a number of microscopic factors may contribute to the strain rate dependency of bulk behavior in syntactic foams.[12] The strain rate sensitivity of the epoxy matrix thanks to the viscoelasticity is one of the key factors to determine the bulk rate dependency of the foam.[22] The stress–strain curves of the pure epoxy resin matrix were measured at the low and high rates; and the representative curves are illustrated in Figure 2. The strain rate sensitivity m of both the syntactic foam ($m_f = 0.082$) and the epoxy matrix ($m_e = 0.106$) was estimated based on the stress (σ) and the strain rate ($\dot{\varepsilon}$) for a given strain state (e.g., $\varepsilon = 0.2$) as follows.[24]

$$m = \frac{\partial \ln \sigma}{\partial \ln \dot{\varepsilon}} \tag{1}$$

The rate dependency of the foam is smaller compared to the epoxy matrix ($m_f < m_e$) probably because (1) the macro-cracking of the matrix occurs earlier in the foam under dynamic compression (as will be discussed below) and (2) the ceramic wall material of cenospheres is less sensitive to the strain rate. Note that the effect of the adiabatic compression of the internal gas may not be expected as a result of (1) the gas drainage through the cracks in the foam and (2) the low initial gas pressure (equal to the atmospheric pressure).

Quasi-static Failure Process: Figure 3 illustrates the internal microstructural change of the syntactic foams that were quasi-statically deformed to different strains and then recovered. The six strain stages were in the plateau region of the compressive response. At the low strain $\varepsilon = 0.1$, some large cenospheres fail in the central portion of the specimen; however, the fragments are adhered to the epoxy matrix walls. After the compressive load is released, the failed cenospheres seem intact due to the recovery of the matrix. Therefore, no obvious internal failure was observed in the foam at the $\varepsilon = 0.1$ in Figure 3. At the increased $\varepsilon = 0.2$, the cenospheres continue to fracture in the central part where the hydrostatic stress is considerable;[12] and the fragments shed off the matrix walls. The spaces (voids) left by the crushed cenospheres become more oblate while the top and bottom portions of the foam specimen seem unchanged (Figure 3). At the high strain $\varepsilon = 0.3$, the crushing of cenospheres occurs along the diagonal of the specimen, in addition to the central part. Meanwhile, macro-cracks can be observed in the epoxy matrix, implying the earlier formation of micro-cracks. At the even higher strains $\varepsilon = 0.4$ to 0.6, the majority of the remaining cenospheres are crushed in the foam. The macro-cracks propagate throughout the specimen and join the voids as well as other cracks, consequently causing the separation of the foam specimen (see $\varepsilon = 0.6$ in Figure 3).

Dynamic Failure Process: Figure 4 shows the μXT observations on the internal failure process of the syntactic foams, which were deformed to different strains in the SHPB tests and then recovered. At the low strain stage ($\varepsilon = 0.1$) of the SHPB compression, the elastic deformation dominates within the foam. However, the fragments of fractured cenospheres can be observed in one side of the foam specimen in the bottom zone of Figure 4 ($\varepsilon = 0.1$). At the increased strains ($\varepsilon = 0.2$ to 0.4) in the plateau region, the two distinct top and bottom zones, as roughly separated by the

dashed lines, become more apparent in the foam (Figure 4). Note that the initial failed ends of the specimens are shown in the bottom of the μXT slices in Figure 4; the failed ends can be either near the input or output bars of the SHPB system. In the bottom zone, the majority of cenospheres are crushed and the macro-cracks evolve in the epoxy matrix. In contrast, most of the cenospheres and the matrix in the top zone remain intact. This implies that the bottom zone deforms plastically whilst the top zone elastically. The similar separation of elastic and plastic zones was also observed in the dynamic deformation of glass microballoon epoxy syntactic foams.[12] When the strain increases, the bottom plastic zone enlarges whereas the top elastic zone reduces (Figure 4). At the high strain $\varepsilon = 0.5$, most cenospheres in the entire foam become crushed; the macro-cracks develop throughout the specimen almost in any directions rather than along a preferential path.

Effect of Strain Rate on Failure Mechanism: The failure process of cenosphere epoxy syntactic foams subjected to quasi-static and dynamic uniaxial compression is dominated by (1) the crushing of cenospheres and (2) the plastic deformation and cracking (micro- and macro-cracking) of the epoxy matrix. These two internal failure processes can be considered the damage in the bulk syntactic foam. The microscopic mechanism in the failure process (i.e., damage evolution) is affected by the strain rate (compare Figure 3 and 4). Figure 5 schematically compares the damage in the foam subjected to quasi-static and dynamic compression. At low strain rates, the damage initiates from the central portion of the foam specimen and then evolves diagonally (Figure 3 and 5). However, under dynamic compression, the damage originates in one end of the specimen and develops towards the other end (Figure 4 and 5). Furthermore, compared to quasi-static compression, macro-cracking of the matrix occurs earlier in the syntactic foam subjected to dynamic loads.

At high strain rates, the load and stress transfer between the two constituents in the syntactic foam is different from that in quasi-static experiments owing to the increased strength of the rate sensitive epoxy matrix. As indicated by the arrows in Figure 4, the macro-cracks can split the cenospheres ahead and propagate through them in the SHPB experiments of the foams. However, splitting of cenospheres by matrix macro-cracking can hardly be observed in the foam subjected to quasi-static compression; instead the macro-cracking in the matrix tends to pass around the cenospheres or debond the cenosphere/matrix interface. The similar phenomena were observed in glass microballoon epoxy syntactic foams by the post-test SEM examination in the previous work.[12,14] However, the present study directly characterized the splitting of cenospheres at the various strain stages in the SHPB compression.

Quantification of Damage Evolution: The damage in the syntactic foam is defined by the failure of cenospheres and the matrix. The damage evolves as a function of both the strain and the strain rate (Figure 3 and 4). In order to quantify the damage, a boundary was specified in the μXT longitudinal slices to contain the crushed cenospheres, the macro-cracks in the matrix and the connection zone between the crushed cenospheres. Figure 5 also schematically shows the representative boundary for the damage at the low and high strain rates. A volume was then reconstructed within the boundaries in these slices to represent the damage in the foam. It should be noted that some intact cenospheres especially in the vicinity of macro-cracks, e.g., the left bottom corner at $\varepsilon = 0.3$ in Figure 4, were included in the damage volume, because the load around these cenospheres was released due to the propagation of the neighboring macro-cracks.

The damage scalar D is defined to be the ratio of the damage volume to the whole specimen volume. Figure 6 illustrates the calculated damage scalar of the deformed foam specimens at various strains and strain rates. An empirical constitutive equation was used to quantify the relation between the damage (D), the strain (ε) and the strain rate ($\dot{\varepsilon}$):[25]

$$D = d \times \dot{\varepsilon}^{(\lambda-1)} \times \left(\varepsilon - \varepsilon_{th}\right)^{n} \qquad (2)$$

where d, λ and n are the material constants, and ε_{th} is the threshold strain for damage initiation. The $\varepsilon_{th} = 0.04$ is estimated based on the measured stress–strain curves (Figure 2). The constants d, λ and n (refer to Table 1) were fitted with a good correlation coefficient $R^2 = 0.9859$. At a given strain, the dynamic damage in the syntactic foam is more severe than the quasi-static damage (Figure 6). Therefore, more energy can be dissipated by the foam under impact condition. Moreover, the foam is completely damaged ($D = 1$) at the lower strain stage under dynamic loads compared to quasi-static compression, implying the reduced ductility at the high rate.

Conclusions: It was found that the failure process in syntactic foams at the quasi-static and dynamic strain rates consists of the crushing of cenospheres and the cracking of the epoxy matrix. However, the microscopic failure mechanism of the foam is significantly influenced by the strain rate. Macro-cracking of the matrix occurs in the earlier strain stage of dynamic compression compared to the quasi-static loading condition. Moreover, at high rates macro-cracks in the matrix can split the cenospheres ahead and propagate through them; however, in quasi-static compression the matrix macro-crack propagates around a cenosphere and does not break it. The damage defined by the failure in the foam can be quantified as a function of the strain and the strain rate using an empirical constitutive equation.

P. Li

Experimental

The Epicote 1006A epoxy resin (matrix) and CENOSTAR ES200/600 cenospheres (hollow ceramic microspheres) were used to fabricate the syntactic foams.[8] The cenospheres were added to the epoxy resin in the multiple steps to obtain a volume fraction of $V = 0.3$; meanwhile the mixture was stirred slowly until it became the uniform slurry. The slurry was then left in a vacuum oven for 10 min to reduce the air bubble introduced by the stir. Subsequently, the mixture was cast in the aluminum molds coated with the release agents and cured for 24 h at room temperature. The cylindrical specimens of the $d = 5$ mm diameter and $l = 5$ mm length were finally machined from the foam.

Uniaxial compression experiments were conducted on the syntactic foam specimens in (1) an INSTRON 5569 mechanical testing machine at the quasi-static strain rate of 0.003 s^{-1} and (2) a split-Hopkinson pressure bar (SHPB) system at the dynamic rate of 3000 s^{-1}. The SHPB system consisted of solid aluminum alloy bars with the 12.7 mm diameter. In some of the quasi-static and dynamic compression tests, the deformation of the foam specimens was controlled to stop at the various strain stages. In quasi-static compression, the different specimens were deformed to the strains $\varepsilon = 0.1, 0.2, 0.3, 0.4, 0.5$ and 0.6. In the SHPB tests, a ring-shaped aluminum stopper was additionally placed around the foam specimen and between the input and output bars to prevent the further deformation of the specimen during the dynamic compression. With the stoppers of different thicknesses, the final deformation of the foam specimens was controlled at the strains $\varepsilon = 0.1, 0.2, 0.3, 0.4$ and 0.5. Note that the lateral deformation (expansion) of the foam specimen was not constrained during

the SHPB compression as the inner diameter (8 mm) of the stopper is larger than the specimen diameter (5 mm).

The syntactic foam specimens deformed to the different strains were then subjected to slow recovery for more than 24 h. Subsequently the x-ray microtomography at 80 kV and 18 μA was performed to scan these specimens.[8,26,27] The effective voxel size was approximately 8 μm. The AVIZO/FIRE software was used to visualize the internal morphology of the foams.

References

[1]   H. Klaus, O. Huber, G. Kuhn, *Adv. Eng. Mater.* **2005,** *7*, 1117.

[2]   R. Huang, P. Li, *Compos. Part B.* **2015,** *78*, 401.

[3]   E.M. Wouterson, F.Y.C. Boey, X. Hu, S.C. Wong, *Compos. Sci. Technol.* **2005,** *65*, 1840.

[4]   J. Gu, G. Wu, Q. Zhang, *Scr. Mater.* **2007,** *57*, 529.

[5]   J. Adrien, E. Maire, N. Gimenez, V. Sauvant-Moynot, *Acta Mater.* **2007,** *55*, 1667.

[6]   F. Awaja, B.D. Arhatari, *Compos. Part A.* **2009,** *40*, 1217.

[7]   E. Maire, N. Gimenez, V. Sauvant-Moynot, H. Sautereau, *Philos. Trans. R. Soc. A.* **2006,** *364*, 69.

[8]   R. Huang, P. Li, T. Liu, *Compos. Struct.* **2016,** *140*, 157.

[9]   I.N. Orbulov, J. Ginsztler, *Compos. Part A.* **2012,** *43*, 553.

[10]   Kishore, S. Kulkarni, D. Sunil, S. Sharathchandra, *Polym. Int.* **2002,** *51*, 1378.

[11]   M. Labella, S.E. Zeltmann, V.C. Shunmugasamy, N. Gupta, P.K. Rohatgi, *Fuel.* **2014,** *121*, 240.

[12]   P. Li, N. Petrinic, C.R. Siviour, R. Froud, J.M. Reed, *Mater. Sci. Eng. A.* **2009,** *515*, 19.

[13]   A. Das, B.K. Satapathy, *Mater. Des.* **2011,** *32*, 1477.

[14]   E. Woldesenbet, S. Peter, *J. Mater. Sci.* **2009,** *44*, 1551.

[15] L. Peroni, M. Scapin, M. Avalle, J. Weise, D. Lehmhus, J. Baumeister, M. Busse, *Adv. Eng. Mater.* **2012,** *14*, 909.

[16] H. Ahmadi, G.H. Liaghat, M.M. Shokrieh, H. Hadavinia, A. Ordys, A. Aboutorabi, *J. Compos. Mater.* **2015,** *49*, 1255.

[17] A. Pellegrino, V.L. Tagarielli, R. Gerlach, N. Petrinic, *Int. J. Impact Eng.* **2015,** *75*, 214.

[18] P. Viot, K. Shankar, D. Bernard, *Compos. Struct.* **2008,** *86*, 314.

[19] Z.Y. Dou, L.T. Jiang, G.H. Wu, Q. Zhang, Z.Y. Xiu, G.Q. Chen, *Scr. Mater.* **2007,** *57*, 945.

[20] M. Veseniak, T. Fiedler, Z. Ren, A. Ochsner, *Adv. Eng. Mater.* **2008,** *10*, 185.

[21] H.S. Kim, H.H. Oh, *J. Appl. Polym. Sci.* **2000,** *76*, 1324.

[22] E. Woldesenbet, N. Gupta, A. Jadhav, *J. Mater. Sci.* **2005,** *40*, 4009.

[23] Z. Wang, P. Li, *AIP Adv.* **2015,** *5*, 16.

[24] P. Li, N.V. Nguyen, H. Hao, *Mater. Des.* **2016,** *89*, 636.

[25] B. Song, W. Chen, *J. Compos. Mater.* **2004,** *38*, 915.

[26] P. Li, N. Petrinic, C.R. Siviour, *Mater. Lett.* **2013,** *100*, 233.

[27] P. Li, *Mater. Sci. Eng. A.* **2015,** *622*, 114.
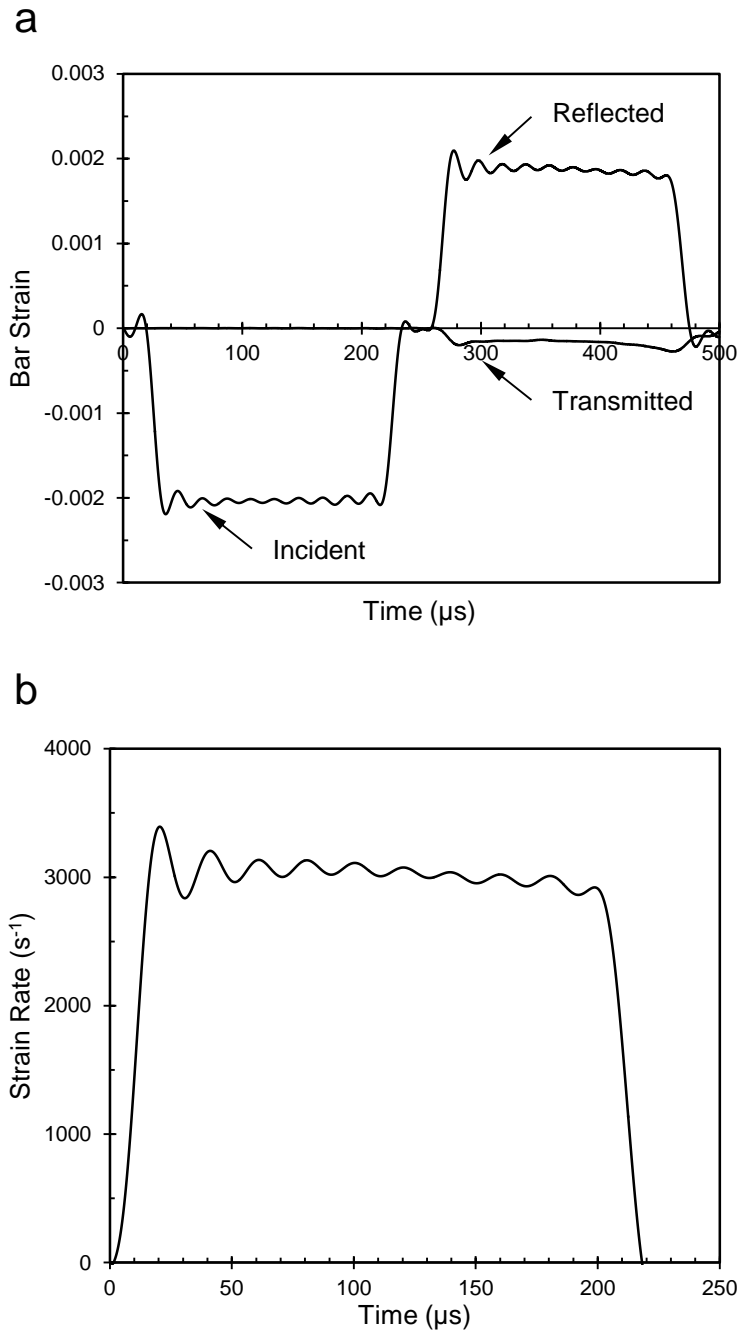
List of Figures

a

b

Fig. 1   The SHPB compression of the cenosphere epoxy syntactic foam: (a) measured strain waves in the bars and (b) calculated strain rate history in the foam specimen.
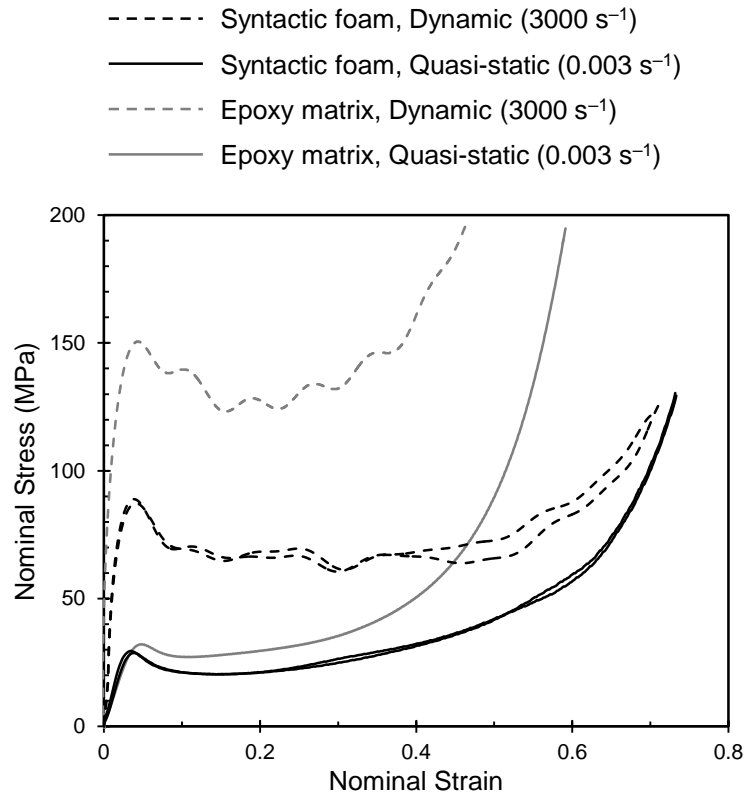
Fig. 2   Representative stress–strain curves of the syntactic foam and the epoxy matrix at the quasi-static and dynamic strain rates.
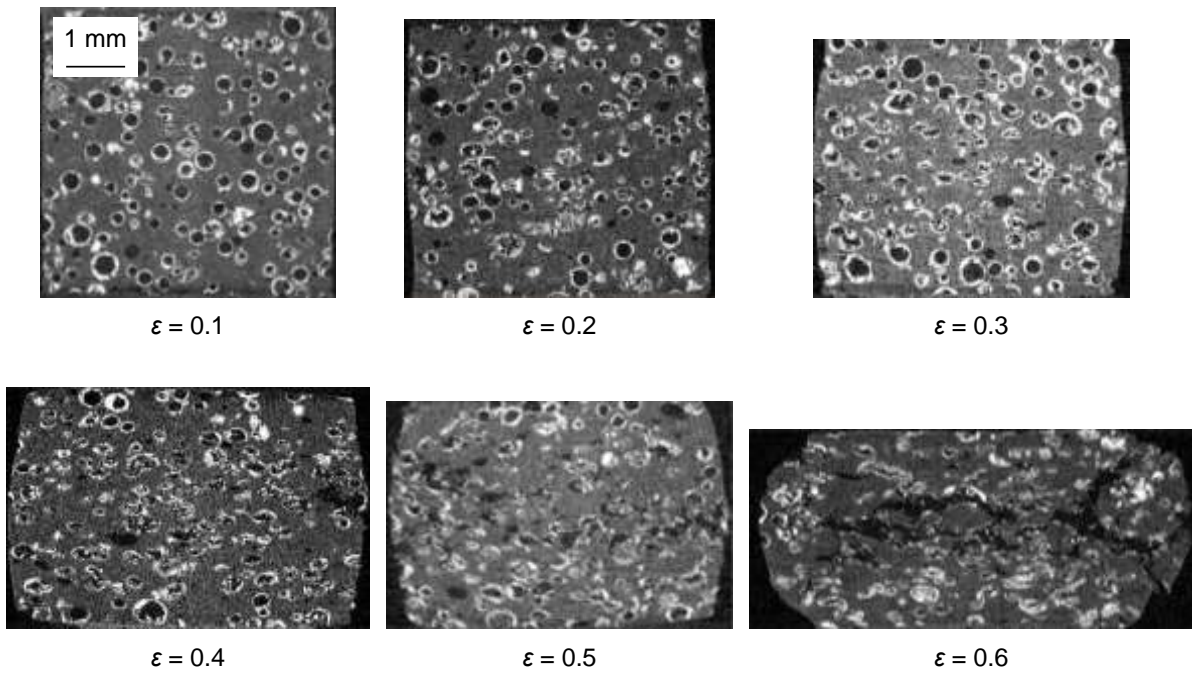
$\varepsilon = 0.1$ $\varepsilon = 0.2$ $\varepsilon = 0.3$

$\varepsilon = 0.4$ $\varepsilon = 0.5$ $\varepsilon = 0.6$

Fig. 3   X-ray microtomographic longitudinal slices of the internal deformation and failure of the syntactic foams at different strain stages of the quasi-static compression.
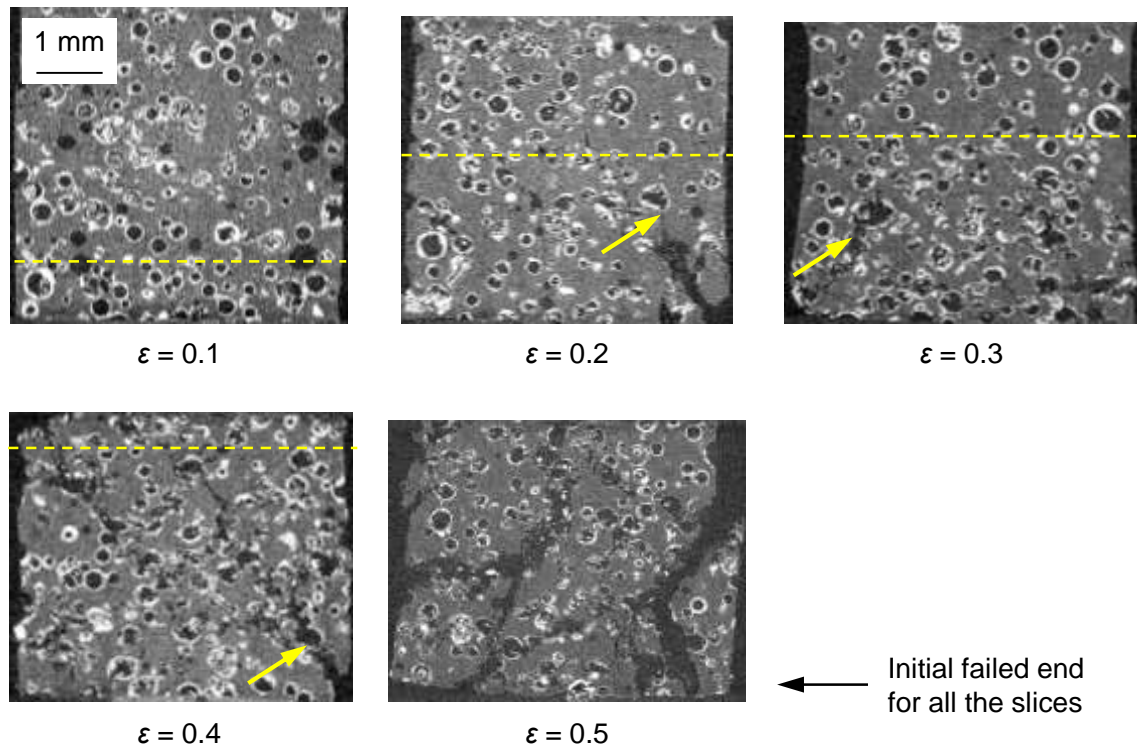
Fig. 4   X-ray microtomographic longitudinal slices of the internal deformation and failure of the syntactic foams at different strain stages of the dynamic compression. (Note: the initial failed end of the foams, which is located at the bottom of each figure, can be either near the input or output bar during the SHPB tests.)
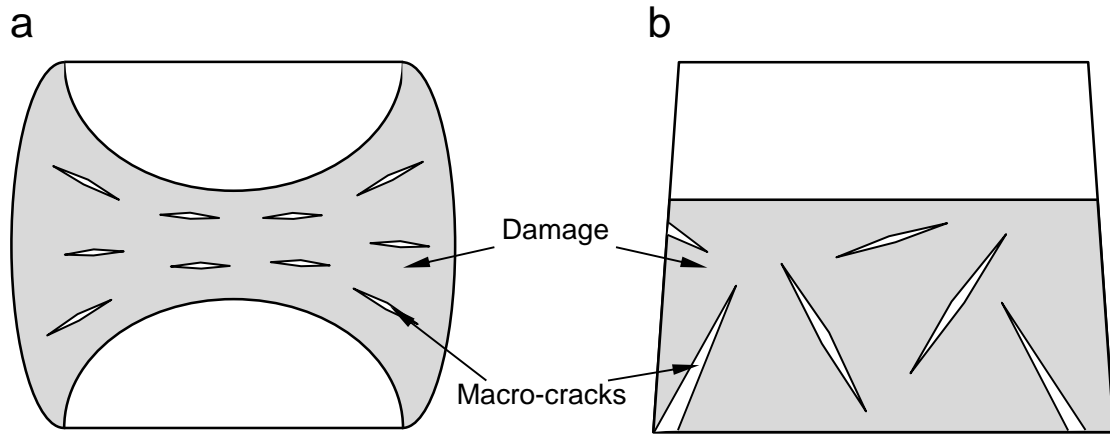
a

b

Damage

Macro-cracks

Fig. 5   The schematic of the damage in the syntactic foam under (a) quasi-static and (b) dynamic compression. (Note: the damage includes the failure of both cenospheres and the matrix.)
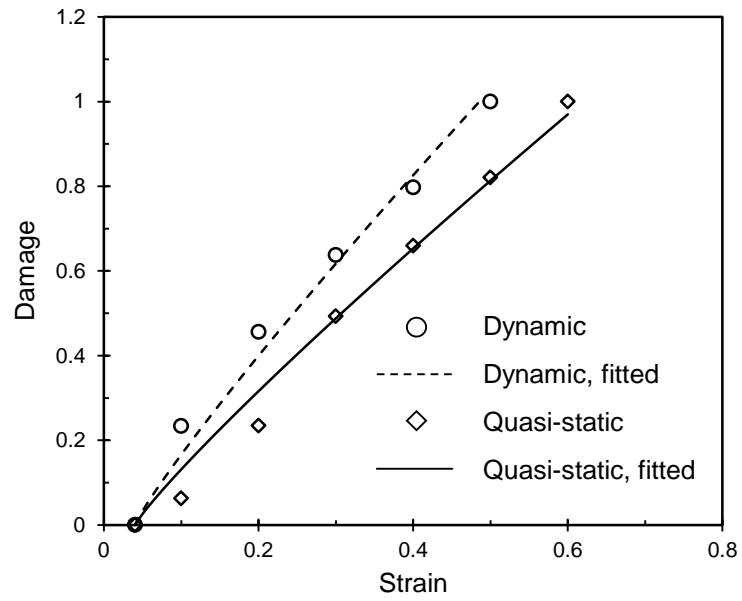
Fig. 6   The damage in the syntactic foam as a function of strains at the quasi-static and dynamic strain rates.

P. Li

List of Tables

Table 1   Constitutive parameters to describe the damage as a function of the strain and the strain rate.

ε_{th}	d	λ	n
0.04	1.805	1.016	0.8947